

Cite this: *Soft Matter*, 2012, **8**, 10226

www.rsc.org/softmatter

## COMMUNICATION

## Structural analysis of “flexible” liposome formulations: new insights into the skin-penetrating ability of soft nanostructures

Oluwatosin A. Ogunsola,<sup>ab</sup> Margaret E. Kraeling,<sup>b</sup> Sheng Zhong,<sup>c</sup> Darrin J. Pochan,<sup>c</sup> Robert L. Bronaugh<sup>d</sup> and Srinivasa R. Raghavan<sup>\*a</sup>

Received 29th March 2012, Accepted 7th August 2012

DOI: 10.1039/c2sm26614h

Self-assembled nanocontainers that can penetrate the protective barrier of skin could prove useful for the needle-free delivery of chemicals, drugs or vaccines into the skin. The main examples of these are the so-called “flexible liposomes”, which are mixtures of lipids and detergents. *In vitro* experiments by numerous researchers have confirmed the skin-penetrating ability of these structures, which is believed to involve the squeezing of flexible bilayers through the pores in the stratum corneum. Here, we reexamine the structure of “flexible” liposome formulations and show that these are actually mixtures of liposomes and micelles. These findings are reinforced through a combination of small-angle neutron scattering (SANS) and cryo-transmission electron microscopy (cryo-TEM). We believe that our new findings necessitate a new mechanism for the penetration of soft assemblies into the skin. Several possibilities in this regard are considered, including one in which micelles facilitate the dynamic exchange of amphiphiles between liposomes and/or lipid bilayers.

## 1. Introduction

The skin is our first line of protection against harmful chemicals and pathogens in the external environment. In particular, the outermost layer of the skin, called the stratum corneum (SC), forms a nearly impermeable barrier to almost all molecules and nanoscale structures.<sup>1–5</sup> Some cosmetic and pharmaceutical companies, however, are interested in finding ways to penetrate the SC, so as to enhance delivery of ingredients into or through the skin. Eventually, for example, this could lead to needle-free vaccination,<sup>6</sup> as well as needle-free supply of insulin to diabetic patients.

Nanoscale containers that could store drugs or vaccines are of special interest for their skin-penetrating ability. One class of such containers are *liposomes*, which are self-assembled structures formed

by lipids, with diameters  $\sim 100$  nm.<sup>7</sup> The SC is known to have small intercellular spaces (20–40 nm) between corneocytes, and these are sometimes called “pores”.<sup>2,3,5</sup> (The use of the term pores in this paper does not refer to other pore pathways of penetration such as hair follicles or sweat ducts.) For liposomes to pass through these pores, the conventional wisdom is that they need to have *flexible* bilayers.<sup>1–5</sup> Flexible liposomes are prepared by combining a lipid, *e.g.*, a phosphatidylcholine (PC) with a denaturant such as a surfactant<sup>1–3</sup> or an alcohol.<sup>4</sup> Surfactants used typically include the nonionic Tween 80 (T80), or the bile salt, sodium cholate (NaC), while ethanol is the alcohol typically used (structures of all three are shown in Fig. 1). Penetration into the skin has generally been assessed using confocal microscopy.<sup>2,4,8</sup>

Cevc and co-workers were the first to show that “flexible” liposomes (which they called Transfersomes®) had the ability to penetrate the SC.<sup>1,2</sup> These liposomes were postulated to squeeze their deformable membranes through the lipidic pores between corneocyte cells. Are these liposomes indeed flexible? The key evidence for flexibility provided in almost every study has been with respect to the permeability of a liposome solution through a filter of much smaller pore size.<sup>1,2</sup> For example, consider the extrusion of 100 nm liposomes through 50 nm pores: if the liposomes were “rigid” (*e.g.*, composed of PC alone), they would clog up the pores and the extrudate would not contain liposomes. In contrast, liposomes of PC + T80 or PC + NaC were shown to be able to pass through the pores, suggesting that the latter had flexible membranes. Apart from permeability experiments, however, little evidence of bilayer flexibility has been reported.<sup>9</sup>

This study began in an effort to measure changes in the bending modulus  $\kappa$  between rigid and flexible liposomes. However, our data have led us to an alternate hypothesis to explain the skin-penetrating ability of liposomes – one that has nothing to do with liposomal flexibility. Our key finding based on data from small-angle neutron scattering (SANS) and cryo-transmission electron microscopy (cryo-TEM) is that the so-called “flexible” liposomes are actually *co-existing mixtures of liposomes and micelles*. Using liposomes of egg-phosphatidylcholine (EPC) and T80, we demonstrate that the liposome samples pass the usual standard for flexibility, *i.e.*, the permeability test through filters. We also conduct *in vitro* skin permeation studies in conjunction with confocal microscopy and show that some structures indeed pass through the SC into the viable epidermis of both hairless guinea pig and human skin. Based on our data, we believe that skin-penetrating liposome formulations contain both

<sup>a</sup>Department of Chemical & Biomolecular Engineering, University of Maryland, College Park, MD 20742, USA. E-mail: sraghava@umd.edu

<sup>b</sup>Center for Food Safety and Applied Nutrition, Food & Drug Administration, College Park, MD 20742, USA

<sup>c</sup>Department of Materials Science & Engineering, University of Delaware, Newark, DE 19716, USA

<sup>d</sup>Consultant, Center for Food Safety and Applied Nutrition, Food and Drug Administration, College Park, MD 20742, USA

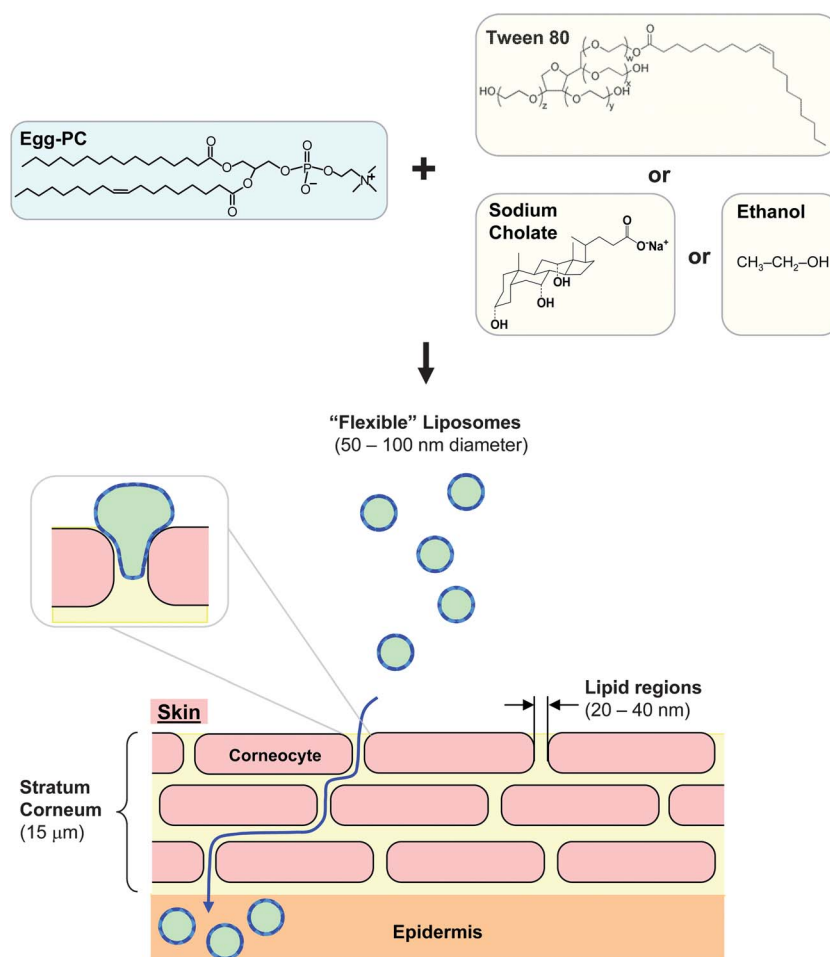


**Fig. 1** "Flexible" liposomes and the conventional mechanism for their action. The liposomes are made by combining a lipid such as egg-PC with a detergent or denaturing agent like Tween 80, sodium cholate, or ethanol (structures of these molecules are shown in the top portion of the figure). The penetration of these liposomes through skin is shown in the bottom part of the figure. The top layer of skin, the stratum corneum (SC), is generally depicted as a "bricks and mortar" structure, with the "bricks" being the corneocyte cells and the "mortar" between the cells composed of lipid multilayers. The liposomes are believed to take a tortuous intercellular route through the lipidic regions (pores) in the SC until they reach the epidermis. Note that the liposomes are bigger than the pores; however, they are believed to be able to squeeze their deformable bilayers through these pores, as depicted in the inset.

liposomes and micelles. This observation is actually consistent with reports in the surfactant literature on many lipid–denaturant mixtures,<sup>10–15</sup> including EPC–NaC,<sup>13–15</sup> however, until now, this point has been ignored in the context of skin permeation. Our findings suggest the possibility that *the co-existence between liposomes and micelles may be critical for penetration through the pores in the stratum corneum*. Possible mechanisms for such penetration are considered later in this paper.

## 2. Experimental section

### Materials

Egg-phosphatidylcholine (EPC) (99% purity) was purchased from Avanti Polar Lipids. Tween 80 (T80) and the fluorescent lipid, 1,*N*-dioctadecyl-3,3,3*N*-tertramethylindocarbocyanine perchlorate (DiI), were purchased from Sigma Aldrich. D<sub>2</sub>O (99.5% deuterated) for the SANS experiments was obtained from Cambridge Isotopes.

### Preparation of liposomal formulations

To a solution of EPC in chloroform, the fluorescent lipid (DiI) was added at a molar ratio of ~1 : 30. The solvent was removed first by exposure to a dry nitrogen stream and thereafter under vacuum in a lyophilizer. An appropriate amount of T80 was then added to the dried lipid film, followed by addition of a pH 7.4 phosphate buffer (0.1 M). The resulting sample was sonicated for 20–30 min to form multilamellar liposomes. The liposomes were then subjected to 4–6 freeze–thaw cycles. Thereafter, the sample was extruded (using a 10 mL Lipex Extruder from Northern Lipids Inc.) through a polycarbonate filter with 100 nm pore size to yield a population of mostly unilamellar liposomes. Different formulations were prepared by varying the molar ratio of detergent to EPC.

### Dynamic Light Scattering (DLS)

DLS was used to characterize the sizes of structures in solution. A Photocor-FC instrument with a 5 mW laser source at 633 nm was

used at a scattering angle of  $90^\circ$ . A logarithmic correlator was used to measure the intensity autocorrelation function. The hydrodynamic diameter of the structure was extracted from the data using the Stokes–Einstein equation.

### Assessments of liposome flexibility by permeation experiments

The vesicles (nominal diameter, 100 nm from DLS) were extruded through three polycarbonate filters with a pore diameter of 50 nm at a pressure of 1724 kPa (250 psi). The amount of the sample passing through the filters during a period of 10 min was weighed. This was normalized with the amount of the sample injected, and the results are expressed as a permeability index  $j$ . An index of 0% implies “rigid”, poorly permeable structures while a value of 100% implies complete permeation and hence “flexible” structures.<sup>1,2</sup>

### SANS

SANS measurements were made on the NG7 and NG3 (30 m) beamlines at NIST in Gaithersburg, MD. The samples were prepared in  $D_2O$  to achieve the needed contrast between the structures in solution and the solvent. The samples were placed in 2 mm quartz cells and studied at  $25^\circ C$ . The scattering spectra were corrected and placed on an absolute scale using calibration standards provided by NIST. The data are shown for the absolute intensity  $I$  versus the wave vector  $q = (4\pi/\lambda)\sin(\theta/2)$ , where  $\lambda$  is the wavelength of incident neutrons and  $\theta$  is the scattering angle.

### SANS data analysis

SANS data were analyzed by the Indirect Fourier Transform (IFT) method, which requires no *a priori* assumptions on the nature of the scatterers.<sup>16–18</sup> Here, a Fourier transformation of the scattering intensity  $I(q)$  is performed to obtain the pair distance distribution function  $p(r)$  in real space.  $p(r)$  provides structural information about the scatterers, such as their shape and maximum dimension. IFT analysis was implemented using the commercial PCG software package.

### CryoTEM

The samples for cryoTEM analyses were prepared using a Vitribot™ system.<sup>19</sup> A droplet of the sample solution (3–5  $\mu L$ ) was placed manually on a copper TEM grid covered with a lacey carbon film. The specimen was then transferred to the Vitribot™, where it was blotted and plunged into a liquid ethane container cooled by liquid nitrogen. The vitrified samples were transferred to a Gatan 626 cryo-holder and thereafter to a Tecnai G2-12 TEM, where they were imaged at a voltage of 120 kV. During TEM observation, the cryo-holder was maintained below  $-170^\circ C$  to prevent sublimation of vitreous water. Digital images were recorded by a Gatan low-dose CCD camera.

### In vitro skin permeation studies

Skin permeation studies were conducted using excised cadaver human skin or hairless guinea pig skin and flow-through diffusion cells.<sup>20–22</sup> Skin diffusion cells (dia.  $0.64\text{ cm}^2$ ) and the perfusion system were prepared for use prior to each study by disinfection with a 70% (v/v) ethanol solution. The diffusion cells were then perfused with

HEPES-buffered Hanks’ balanced salt solution (Life Technologies), which was used as the receptor fluid. Discs of dermatomed (250–400  $\mu m$ ) skin were obtained using a punch (17 mm) and each disc was then mounted in the diffusion cell with the epidermal side up. The skin surface temperature was maintained at  $32 \pm 2^\circ C$  by circulating  $35 \pm 2^\circ C$  water through a diffusion cell-holding block. The diffusion cell-mounted skin was allowed to equilibrate for at least 30 min with the pumping of receptor fluid at a flow rate of about  $1.5\text{ mL h}^{-1}$ . After 30 min, 10  $\mu L$  of the various liposomal formulations were non-occlusively applied to the top surface of the skin. A minimum of two diffusion cells per experiment were run for each formulation type and exposure. Each formulation type was tested on the skin from 2–4 guinea pigs or humans ( $n = 4–8$ ). Receptor fluid fractions were collected at 6 h intervals for a total of 24 h using a fraction collector. After 24 h, the experiment was stopped and the middle sections of each skin disc were cut, snap frozen in liquid nitrogen, and embedded in Tissue-Tek optimal cutting temperature (OCT) media, purchased from Sakura Finetek. Slices (10–20  $\mu m$ ) of the frozen skin were cut in a cryostat (Reichert-Jung 2800 Frigocut). These samples were then analyzed for penetration of DiI using a laser scanning confocal microscope (Zeiss 510 UV LSM confocal microscope, 543 nm laser line, 1% power attached to an Axiovert 100M Inverted Microscope, 40 $\times$  objective).

## 3. Results and discussion

### Liposomal formulations: extrusion measurements

Our initial studies sought to verify typical results on “flexible” liposomes prepared by combining EPC with T80. Our controls, *i.e.*, “rigid” liposomes of  $\sim 100$  nm diameter, were made with 13 mM EPC (1 wt%). The mixtures were prepared by combining the above EPC with varying amounts of T80. Compositions are denoted by the mol percent; of T80 therein. The usual test for assessing liposomal “flexibility” is to extrude the 100 nm liposomes through filters of smaller pore size<sup>1–5</sup> – in our case, 50 nm. Table 1 reports the permeability index  $j$  (percent of injected solution that extrudes out in a given time at a given pressure) for the various formulations. As expected,  $j$  is low for the “rigid” liposomes (100% EPC, 0% T80), indicating that these are unable to penetrate through fine pores.  $j$  increases substantially as the mol% T80 in the formulation increases. The samples with 46% or more of T80 extruded almost completely through the fine pores and so their  $j$  values are nearly identical. The

**Table 1** Size and permeability measurements on liposome and vesicle samples

Sample composition <sup>a</sup>	Hydrodynamic diameter $D_h^b$ (nm)	Permeability index $j^c$ (%)
EPC	110	3%
EPC + T80 (9%)	104	80%
EPC + T80 (37%)	104	80%
EPC + T80 (46%)	92	94%
EPC + T80 (68%)	99	100%
EPC + T80 (77%)	74	100%

<sup>a</sup> In the case of the EPC–T80 samples, each sample contains 13 mM of EPC and varying amounts of T80; the mol% of T80 in each mixture is indicated. <sup>b</sup> Measured using DLS. <sup>c</sup> Measured by extruding samples through filters with pores of 50 nm diameter. The index corresponds to the percent of injected fluid that extrudes through the filters over a period of 10 min at an applied pressure of 1724 kPa (250 psi).

extrusion test confirms that EPC–T80 liposomes are “flexible” according to the conventional standard.

### Liposomal formulations: *in vitro* skin penetration studies

We then proceeded to examine the skin penetration of EPC–T80 mixtures. For these tests, the amount of EPC was increased to 26 mM (2 wt%) and the T80 amount was increased as well. The samples are again labeled according to their T80 mol%. The fluorescent lipid, DiI, was included to allow for imaging by confocal microscopy. *In vitro* tests were conducted with both hairless guinea pig skin (Fig. 2A) and excised human skin (Fig. 2B). Each formulation was applied non-occlusively for 24 h, and the images shown are for cross-sections of washed skin samples. Note that the fluorescence is confined to the SC in the case of formulations containing either EPC alone (images A1, B1), a small (25%) amount of T80 (image A2), or T80 alone (image B3). On the other hand, bright fluorescence throughout the SC and into the epidermis was seen for formulations with 46% or more of T80. Representative examples are shown for 60% T80 with guinea pig skin (image A3) and 68% T80 with human skin (image B2). The above skin penetration experiments are entirely consistent with the original findings of Cevc and other researchers,<sup>1–5</sup> many of whom have studied the very same combination of EPC–T80. To summarize, liposomes of EPC alone are unable to pass through either fine pores in the filter or through the SC in skin. Mixtures of EPC and T80, on the other hand, show considerable penetration through both these semipermeable barriers. The question is whether these results truly reflect differences in flexibility between the liposomal bilayers in the two cases.

### Liposomal formulations: SANS

Next, we examined EPC–T80 solutions using SANS (samples in D<sub>2</sub>O, compositions identical to those in Table 1). The master plot in Fig. 3a shows SANS spectra (intensity  $I$  vs. wave vector  $q$ ) for six different samples. The pure EPC sample reveals the characteristic signature of liposomes, which is a decay of the intensity with a slope of  $-2$  on the log–log plot (*i.e.*,  $I \sim q^{-2}$ ).<sup>18,23</sup> At the other extreme, the sample of 77% T80 shows the signature of spherical micelles, which is a plateau in intensity at low  $q$  and a smooth curvature at high  $q$ .<sup>18,23</sup> Between these extremes, the samples with intermediate T80 content (9 to 68%) exhibit characteristic features of both liposomes and micelles. Note that, as the % of T80 increases, the intensity drops at low  $q$  and increases at high  $q$ . Moreover, the curvature of the plot at high  $q$  steadily increases until it coincides with the “micellar” curve. To illustrate this clearly, the plot of a particular sample with 68% T80 is compared in Fig. 3b with the plot for EPC liposomes—both plots show a slope of  $-2$  at low  $q$ , indicating a contribution from liposomes. The same plot is compared in Fig. 3c with that for 77% T80 (micelles) and the plots now almost exactly coincide at moderate to high  $q$ —indicating a substantial contribution from micelles.

To further establish the co-existence of liposomes and micelles, we resorted to analyzing our SANS data using the Indirect Fourier Transformation (IFT) method.<sup>16–18</sup> The advantage with this analysis is that no *a priori* assumptions are made about the type of structure existing in the sample. Using IFT, the  $I(q)$  data is Fourier-transformed to yield a pair distance distribution function  $p(r)$  in real space.<sup>16</sup> For reference, we show in Fig. 4a the typical  $p(r)$  signatures for spherical micelles, cylindrical micelles and liposomes.<sup>16,17</sup> The  $p(r)$

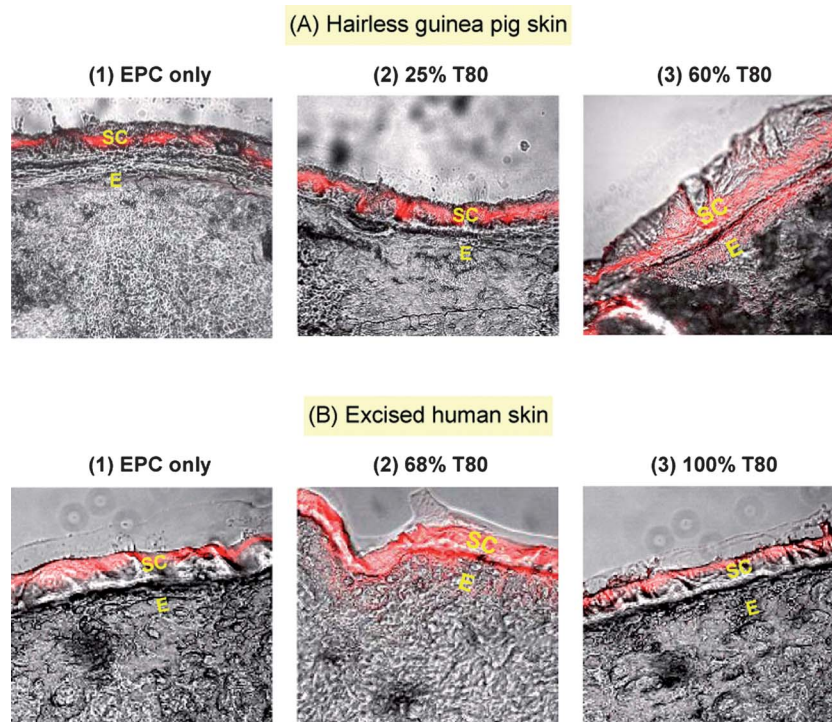


**Fig. 2** Confocal microscopy images showing indirect evidence for the penetration of EPC–T80 liposomes into the epidermis of (A) hairless guinea pig skin; and (B) excised human skin. On the one hand, liposomes of EPC alone (A1, B1) or with low amounts of T80, *e.g.*, 25 mol% (A2), do not penetrate much into either type of skin. Similarly, micelles of T80 also penetrate negligibly (B3). On the other hand, the samples containing 60% T80 (A3) and 68% T80 (B2) are both able to penetrate significantly through the stratum corneum (labeled SC) and into the epidermis (labeled E). Note that the structures are tagged with the fluorescent lipid DiI, and therefore the presence of red fluorescence in the epidermal layer reflects the presence of liposomes.

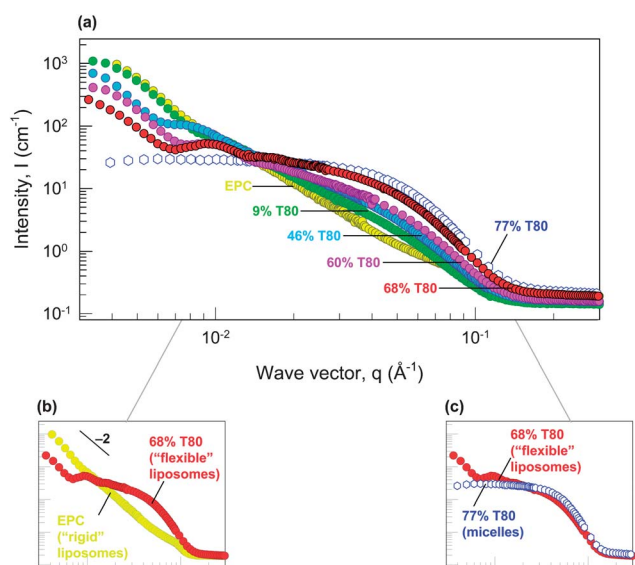


**Fig. 3** (a) SANS scattering at 25 °C from formulations containing EPC and T80. Each formulation contains 13 mM of EPC and varying amounts of T80. The mol% of T80 in each sample is indicated on the plot. The scattering profiles for 46%, 60%, and 68% T80 are intermediate between those for micelles and liposomes. To illustrate this more clearly, (b) compares the data for the 68% T80 sample with that for EPC liposomes (0% T80). Note the similarities in the two spectra at low  $q$  (slope close to  $-2$ , which is characteristic of liposomes). Next, (c) compares the same data with that for 77% T80, which is a typical scattering pattern for spherical micelles. Note the similarities between the two sets of data at moderate and high  $q$ .

of liposomes is symmetrical with a single, broad peak and this matches with the  $p(r)$  for the pure EPC sample in Fig. 4b. Conversely, the  $p(r)$  for spherical micelles is a narrow distribution with a single, sharp peak and this matches with the  $p(r)$  for the 77% T80 sample. Consider now the samples with intermediate T80 content. For 46% and 60% T80, the  $p(r)$  does not follow any of the simple patterns from Fig. 4a. Rather, both these curves have a double moded distribution, *i.e.*, a shoulder and a peak—which is a possible indication of *co-existing structures*.<sup>17,18</sup> Interestingly, the shoulder of the 46% plot turns into a peak in the 60% T80 plot and both occur at low  $r$ , much like the peak of the 77% T80 (micellar) plot. This confirms that micelles are one of the structures in the samples and that the proportion of micelles increases with increasing T80 content.

To summarize, the IFT modeling confirms the co-existence of micelles and liposomes in samples containing an appreciable amount of T80 along with EPC. Note that by using the IFT technique, we are able to reach the above conclusion without making *a priori* assumptions about the type(s) of structure(s) present. Further direct modeling of the SANS data requires superposition of scattering functions from vesicles and from micelles—for this, the shapes of the micelles as well as their relative volume fraction need to be known or assumed. Such modeling is not attempted here, but our results from cryo-TEM (see below) offer additional insight into the structures present.

### Liposomal formulations: cryo-TEM

To independently confirm the co-existence of structures in EPC–T80 samples, we resorted to cryo-TEM. In this technique, the structures in

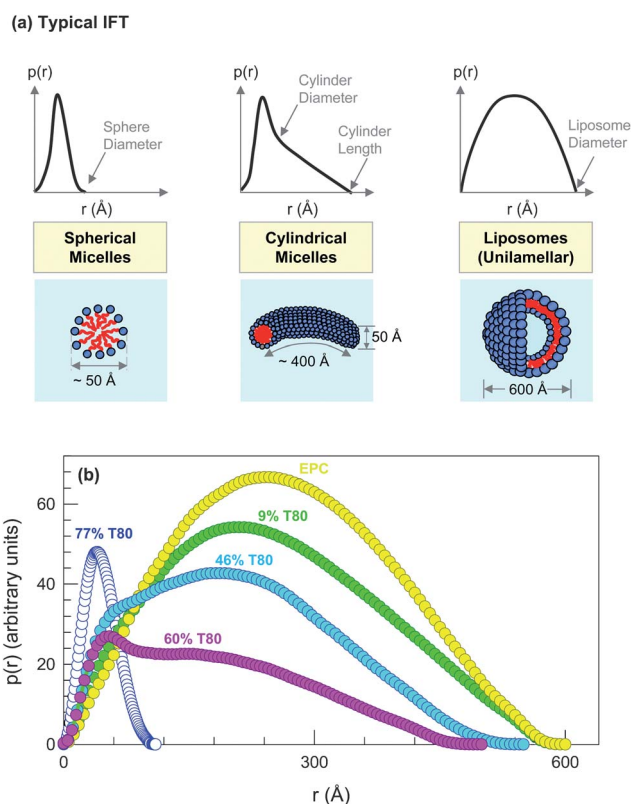


**Fig. 4** IFT analysis of the SANS data in Fig. 3. For reference, (a) illustrates the typical IFT results for spherical micelles, cylindrical micelles, and liposomes. In our case, note that the IFT plots in (b) for 77% T80 and 9% T80 are both characteristic of liposomes, while the plot for 77% T80 is indicative of spherical micelles. On the other hand, the IFT plots for the 46% and 60% T80 samples show both a peak and a shoulder: these are not indicative of any single type of structure; rather they imply a *coexistence* of micelles and liposomes in the samples.

solution are preserved by rapid freezing.<sup>10,24</sup> Fig. 5 shows representative images of samples containing (a) EPC only and (b) EPC–T80 with 46% T80. The EPC sample (Fig. 5a) is composed entirely of liposomes, which is consistent with the SANS analysis. The EPC–T80 sample also contains many liposomes, but in co-existence with these liposomes, we also see a number of dark lines or curves, highlighted using blue arrows. These are *disklike micelles* (also sometimes called bilayered micelles or bicelles),<sup>25–28</sup> and they are known intermediates between micelles and liposomes.<sup>19,29,30</sup> As noted in previous cryo-TEM studies, the disks are seen edgewise in the images, which is why they appear as dark, thick lines (also they appear with much higher contrast compared to cylindrical micelles).<sup>19</sup> Their diameters are around 100–200 nm and their thickness is comparable to that of the liposomal bilayers. The samples with higher T80 content were also analyzed using cryo-TEM and similar findings were obtained for those as well. In the case of the 68% T80 sample (images not shown), only a few liposomes could be observed and these were in co-existence with a few disklike micelles as well as a large number of smaller spherical micelles ( $\sim 5$  to 10 nm). As expected, spherical micelles were also observed by cryo-TEM in samples of pure T80. In summary, cryo-TEM provides direct, “real-space” evidence for co-existing populations of liposomes and micelles in EPC–T80 solutions with 46% to 68% of T80. The cryo-TEM results thereby corroborate the findings from SANS.

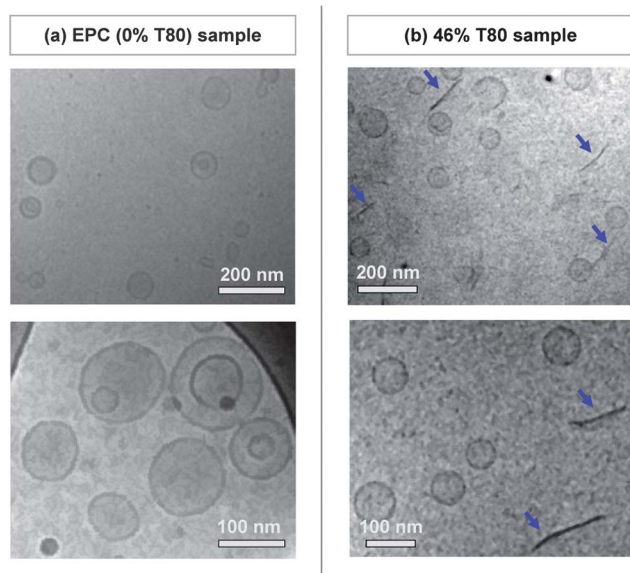


**Fig. 5** Cryo-TEM images of formulations corresponding to “rigid” and “flexible” liposomes. The former contains 13 mM EPC alone and its images, shown in (a), reveal a number of liposomes that are either unilamellar or bilamellar. The latter is a mixture of 13 mM EPC and 11 mM T80 (molar ratio of T80 = 46%) and its images in (b) reveal a combination of spherical unilamellar liposomes and a number of disklike micelles (marked by arrows). The disks are seen from the side, which is why they show up as dark lines or curves in the images.

A stable co-existence between liposomes (vesicles) and micelles has been reported before in a number of lipid–detergent mixtures.<sup>10–15</sup> In particular, we wish to highlight a cryo-TEM study by Walter *et al.*<sup>13</sup> on mixtures of EPC and NaC. *The image of the 40 mol% NaC sample (Fig. 4a of their paper) is remarkably like those of the EPC–T80 sample in Fig. 5b: it shows liposomes in co-existence with disklike micelles.* Another sample with 42 mol% NaC (Fig. 4c of their paper) also showed a co-existence, this time between liposomes and short cylindrical micelles. SANS studies on EPC–bile salt samples have also inferred a vesicle–micelle co-existence.<sup>14,15</sup> Altogether, we can conclude that the two most popular “flexible” liposome formulations (EPC–T80 and EPC–NaC) are both combinations of liposomes and micelles.

### Possible mechanisms for skin penetration

If “flexible” liposomes are indeed combinations of liposomes and micelles, it is possible that the co-existing micelles have a central role to play in skin penetration. In other words, it is possible that skin penetration occurs by an alternate mechanism not involving liposomal flexibility. Note that any alternate mechanism will have to explain why a sample such as EPC–T80 is able to pass through *both* the pores in the filter as well as those in the SC, whereas a control sample of EPC alone is not. It is also worth reiterating that the fluorescent marker used here, *i.e.*, DiI, is a lipid with two octadecyl tails and it is insoluble in water or buffer. Thus DiI cannot penetrate through skin unless it is associated with amphiphiles, such as in a lipid membrane. Below, we consider three possible mechanisms to explain our results.

### Mechanism 1

The first possibility is that the micelles are “clearing the path” for liposomes by solubilizing the skin lipids in the pores.<sup>29</sup> In other words, the role of the micelles is to disrupt the integrity of the multilamellar lipid bilayers present in the pores so that there is less of a barrier for liposomal transport. While this mechanism seems plausible, one point to note is that we also observed permeation of liposome–micelle mixtures through the fine pores of a polycarbonate filter. In the latter case, the micelles cannot possibly be solubilizing the polycarbonate material. So while this mechanism can explain penetration through skin, it cannot account for penetration through the filter.

### Mechanism 2

A second possibility is that in a liposome–micelle mixture, it is the micelles (not the liposomes) that are actually the skin-penetrating structures. Clearly, micelles can be small enough (<10 nm) to pass through fine pores. However, in our own experiments, pure micelles (*e.g.*, 100% T80) showed only weak penetration through skin compared to EPC–T80 mixtures. There have also been several studies that have examined micellar solutions on skin and these have not found unusual levels of penetration for these structures.<sup>31,32</sup> Thus, this mechanism also appears to be inconsistent with the data.

### Mechanism 3

A third possibility is one in which *micelles facilitate the dynamic exchange of amphiphiles between liposomes and/or the lipid bilayers* of skin, and thereby facilitate the penetration of liposomes through pores in both the filter and the SC. Exchange of lipids between liposomes generally occurs very slowly (~minutes to hours) due to the low solubility of lipids in water.<sup>7,33</sup> On the other hand, exchange of amphiphiles among micelles occurs rapidly (~milliseconds).<sup>33</sup> In mixtures like EPC–T80, micelles enriched in T80 (but containing some EPC) will co-exist with liposomes enriched in EPC (but containing some T80). We speculate that the exchange of amphiphiles between such co-existing micelles and liposomes occurs quite rapidly. This may be able to explain permeation through both filter pores and skin pores.

First consider an EPC–T80 liposome–micelle mixture being extruded through filter pores. Initially, the small mixed micelles will pass through the pores, carrying some of the EPC molecules along.<sup>34</sup> Because the structures can exchange rapidly, osmotic gradients can come into play,<sup>35,36</sup> and this can drive more of both EPC and T80 to the extrudate side. Note that the structures in EPC–T80 are “fluid”—implying that they do not retain a particular form indefinitely (this is a classic feature of self-assembly).<sup>33</sup> In contrast, pure EPC liposomes are akin to “solid” entities rather than self-assemblies. Their slow dynamics precludes them from crossing fine pores.

Next, consider the penetration of EPC–T80 samples in contact with skin pores, *i.e.*, the lipid multilayers between corneocytes. We speculate a rapid dynamic exchange of amphiphiles between the structures: for example, lipids in the skin can incorporate into the micelles or liposomes, while EPC lipids can fuse and become a part of the skin bilayers. This dynamic exchange may allow lipids from the liposomes and micelles to insert into the multilayers. Once again, the presence of the micelles is postulated to be critical for speeding up the dynamics of the process; *i.e.*, it will not occur for the case of liposomes of pure EPC because the dynamics (in the absence of

micelles) is too slow. Also, in this process, it is not clear if the liposomes remain intact or if they break and get reconstituted multiple times. If the liposomes do substantially fragment as they permeate through skin, it has implications for delivery of a solute encapsulated in the liposomal interior. Such a solute may be released prematurely in the outer layers of the skin, *i.e.*, much of the solute may not reach the deeper epidermis.

We conclude this section by reiterating that more evidence is necessary to discriminate between the various possible mechanisms. Regardless of the correct mechanism, it is possible and even likely that the presence of co-existing micelles is critical to skin penetration of liposomes, a point that has been ignored in previous studies.

#### 4. Conclusions

In summary, our study proposes that the penetration of liposomal samples into skin may be associated, not with the flexibility of the structures, but with the simultaneous presence of liposomes and micelles. The coexistence of these two structures is an outcome of the sample compositions, *i.e.*, typically being mixtures of a lipid and a detergent. The role of micelles in skin penetration may be through their ability to facilitate the dynamic exchange of amphiphiles between the assemblies, *i.e.*, in making the assemblies “fluid”. More studies will be needed to clarify the nature of the penetration mechanism. Ultimately, a new mechanism can lead to the design of new formulations having unique capabilities of penetrating skin, and thus moving us a step closer to the transdermal delivery of drugs or vaccines.

#### 5. Disclaimer

The views expressed in this manuscript are those of the authors alone. They do not represent the views or opinions of the US FDA or any entity of or affiliated with the US FDA. The contents of this manuscript do not imply any endorsement or disapproval of the use of the nanomaterials mentioned herein.

#### Acknowledgements

This work was funded by a grant from JIFSAN and an ORISE fellowship to OAO. We acknowledge NIST for facilitating the SANS experiments performed as part of this work. We also acknowledge Dr Hee-Young Lee and Dr Matthew Dowling for assistance with the formulation studies and modeling, Dr Li Komatsu and Dr Li Mu for assistance with the skin penetration studies, and Amy Beaven for guidance in using the confocal microscope.

#### References

- G. Cevc, A. Schatzlein and G. Blume, *J. Controlled Release*, 1995, **36**, 3–16.
- G. Cevc, *Adv. Drug Delivery Rev.*, 2004, **56**, 675–711.
- J. A. Bouwstra, P. L. Honeywell-Nguyen, G. S. Gooris and M. Ponec, *Prog. Lipid Res.*, 2003, **42**, 1–36.
- E. Touitou, N. Dayan, L. Bergelson, B. Godin and M. Eliaz, *J. Controlled Release*, 2000, **65**, 403–418.
- G. M. Maghraby, B. W. Barry and A. C. Williams, *Eur. J. Pharm. Sci.*, 2008, **34**, 203–222.
- G. M. Glenn, D. N. Taylor, X. R. Li, S. Frankel, A. Montemarano and C. R. Alving, *Nat. Med.*, 2000, **6**, 1403–1406.
- A. Jesorka and O. Orwar, *Annu. Rev. Anal. Chem.*, 2008, **1**, 801–832.
- D. D. Verma, S. Verma, G. Blume and A. Fahr, *Eur. J. Pharm. Biopharm.*, 2003, **55**, 271–277.
- B. A. I. van den Bergh, P. W. Wertz, H. E. Junginger and J. A. Bouwstra, *Int. J. Pharm.*, 2001, **217**, 13–24.
- M. Almgren, K. Edwards and G. Karlsson, *Colloids Surf., A*, 2000, **174**, 3–21.
- K. Edwards, J. Gustafsson, M. Almgren and G. Karlsson, *J. Colloid Interface Sci.*, 1993, **161**, 299–309.
- M. Silvander, G. Karlsson and K. Edwards, *J. Colloid Interface Sci.*, 1996, **179**, 104–113.
- A. Walter, P. K. Vinson, A. Kaplun and Y. Talmon, *Biophys. J.*, 1991, **60**, 1315–1325.
- S. U. Egelhaaf and P. Schurtenberger, *Phys. Rev. Lett.*, 1999, **82**, 2804–2807.
- M. A. Long, E. W. Kaler and S. P. Lee, *Biophys. J.*, 1994, **67**, 1733–1742.
- O. Glatter, *J. Appl. Crystallogr.*, 1977, **10**, 415–421.
- F. P. Hubbard, G. Santonicola, E. W. Kaler and N. L. Abbott, *Langmuir*, 2005, **21**, 6131–6136.
- T. S. Davies, A. M. Ketner and S. R. Raghavan, *J. Am. Chem. Soc.*, 2006, **128**, 6669–6675.
- Y. Xia, I. Goldmints, P. W. Johnson, T. A. Hatton and A. Bose, *Langmuir*, 2002, **18**, 3822–3828.
- R. L. Bronaugh and R. F. Stewart, *J. Pharm. Sci.*, 1985, **74**, 64–67.
- M. E. K. Kraeling and R. L. Bronaugh, *J. Soc. Cosmet. Chem.*, 1997, **48**, 187–197.
- OECD Guidance document no. 28 for the conduct of skin absorption studies, 2004, [http://apli1.oecd.org/olis/2004doc.nsf/linkto/env-jm-mono\(2004\)2](http://apli1.oecd.org/olis/2004doc.nsf/linkto/env-jm-mono(2004)2).
- J. S. Pedersen, *Adv. Colloid Interface Sci.*, 1997, **70**, 171–210.
- H. Cui, T. K. Hodgdon, E. W. Kaler, L. Abezgauz, D. Danino, M. Lubovsky, Y. Talmon and D. J. Pochan, *Soft Matter*, 2007, **3**, 945–955.
- L. van Dam, G. Karlsson and K. Edwards, *Biochim. Biophys. Acta, Biomembr.*, 2004, **1664**, 241–256.
- J. Katsaras, T. A. Harroun, J. Pencer and M. P. Nieh, *Naturwissenschaften*, 2005, **92**, 355–366.
- L. Barbosa-Barros, A. de la Maza, J. Estelrich, A. M. Linares, M. Feliz, P. Walther, R. Pons and O. Lopez, *Langmuir*, 2008, **24**, 5700–5706.
- L. Barbosa-Barros, C. Barba, G. Rodriguez, M. Cocera, L. Coderch, C. Lopez-Iglesias, A. de la Maza and O. Lopez, *Mol. Pharmaceutics*, 2009, **6**, 1237–1245.
- J. Lasch, *Biochim. Biophys. Acta, Rev. Biomembr.*, 1995, **1241**, 269–292.
- J. Leng, S. U. Egelhaaf and M. E. Cates, *Biophys. J.*, 2003, **85**, 1624–1646.
- P. N. Moore, S. Puvvada and D. Blankschtein, *J. Cosmet. Sci.*, 2003, **54**, 29–46.
- P. N. Moore, A. Shiloach, S. Puvvada and D. Blankschtein, *J. Cosmet. Sci.*, 2003, **54**, 143–159.
- D. F. Evans and H. Wennerstrom, *The Colloidal Domain: Where Physics, Chemistry, Biology, and Technology Meet*, Wiley-VCH, New York, 2001.
- K. Morigaki, P. Walde, M. Misran and B. H. Robinson, *Colloids Surf., A*, 2003, **213**, 37–44.
- G. Cevc and D. Gebauer, *Biophys. J.*, 2003, **84**, 1010–1024.
- G. Cevc, A. G. Schatzlein, H. Richardsen and U. Vierl, *Langmuir*, 2003, **19**, 10753–10763.